

Influence of Agglomerates of Conducting Spheres on the Response of a Phase-Doppler Anemometer

Adrian Doicu*, Gerhard Göbel*, Thomas Wriedt**, Klaus Bauckhage*

Dedicated to Professor Dr. Heinz Fissan on the occasion of his 60th birthday

(Received: 25 January 1998; resubmitted: 31 July 1998)

Abstract

The influence of agglomerates of solid conducting spheres on the response of a phase-Doppler anemometer (PDA) is described for a two-sphere system by using a ray theory model. First- and second-order reflection and diffraction are considered for far-field calculations of the PDA phase

difference. The numerical simulations are accompanied and supported by experimental results. Two-sphere systems of *Sn63Pb37* alloy particles were captured inside an electrodynamic trap and investigated with a standard phase-Doppler system.

1 Introduction

Disperse systems represent a significant component of a large variety of processes of industrial relevance. Precise knowledge of the particle size distribution is of great importance in order to yield optimal performance. Laser-optical techniques are often preferred owing to their ability to perform non-intrusive particle characterization. Phase-Doppler anemometry (PDA) is one of these well established techniques. Similarly to other techniques, PDA suffers from the fact that its response is sensitive to deviations of the particle shape and particle surface from the spherical shape and smooth surface assumed in the underlying light scattering theory. Theoretical work concerning the response of a PDA to rough spherical particles, supported by experimental results on individual rough spheres, has been published recently [1].

Another type of deviation from the ideal particle properties that occur in industrial applications is the formation of agglomerates due to various types of forces between particles. It is of interest to gain knowledge about the possible impact of agglomeration on the response of a sizing technique.

Electromagnetic scattering by an ensemble of particles has been the subject of numerous studies in optics. Rigorous solutions for computing the electromagnetic scattering from spheres by taking into account the coupling among particles have been reported by *Trinks* [2], *Bruning and Lo* [3], *Borghese et al.* [4], and *Fuller and Kattawar* [5]. However, the complexity of the problem has thwarted efforts to obtain numerical results for all but a few small spheres. The root of the difficulty could be traced to two features of the solution schemes in the previous methods. The first is that all the previous methods are based on a brute-force method in which an \mathcal{N} -sphere scattering solution is solved at once. Consequently, the matrix equation of the scattering problem becomes large and owing to the considerable computational effort the number and the

size parameters of the spheres are limited. This problem was partially solved by *Wang and Chew* [6] by using a generalized recursive aggregate T-matrix approach for solving the \mathcal{N} -sphere scattering problem recursively. The second difficulty is associated with the calculation of the coefficients of the vector addition theorem in three dimensions. Equations for the calculation of the vector addition theorem in three dimensions were derived by *Stein* [7] and *Cruzan* [8]. These equations require the calculation of many Wigner 3-j coefficients, which involve a large number of factorials. From a computational viewpoint, this is a very inefficient method.

Another disadvantage of exact methods is they give little physical insight into the scattering mechanism behind the resulting scattered intensity distribution. On the other hand, approximate methods can give a clear picture of the physical process involved in the scattering. Furthermore, for large size parameters, the approximate methods for calculating the far-field scattered intensity have superior computational efficiency to the rigorous methods. One of these approximate methods is the ray theory. The ray theory or the geometric optics model gives a good approximation of the far-field intensity in the forward scattering hemisphere. The higher computational speed makes it economically viable to compute the amplitude and phase of the scattered light over a fine grid on the receiver aperture.

The aim of this paper is to model the phase Doppler signal for a two-sphere system by using an approximate geometric optics model. The purpose is to check the range of applicability of the ray theory and in particular to give a clear picture of the influence of the agglomeration process on the response of a PDA. For the case of reflecting spheres in a PDA system we used a geometric optics model accounting for specular reflection and diffraction. Measurements on an electrostatically levitated agglomerate built of two *Sn63Pb37* alloy particles supports the theoretical results.

2 Specular Reflection Model for Computing the Doppler Signal Phase

We consider two perfectly conducting spheres of radii a_1 and a_2 and denote by Δ the distance between their centers O_1 and O_2 . We

* Dr.-Ing. A. Doicu, Dr.-Ing. G. Göbel, Prof. Dr.-Ing. K. Bauckhage, Fachgebiet Verfahrenstechnik, Universität Bremen, Badgasteiner Straße 3, 28359 Bremen (Germany).

** Dr.-Ing. T. Wriedt, Institut für Werkstofftechnik, Badgasteiner Straße 3, 28359 Bremen (Germany).

choose a local coordinate system O_1xyz having the origin located at the point O_1 . The orientation of the z -axis with respect to a global coordinate system O_1XYZ is given by the Euler angles α and β . The particles are illuminated by a monochromatic plane wave travelling in the $\mathbf{e}_i(\varphi_i, \theta_i)$ direction. The azimuthal angles are specified in the global coordinate system. The geometry of the scattering problem is shown in Figure 1.

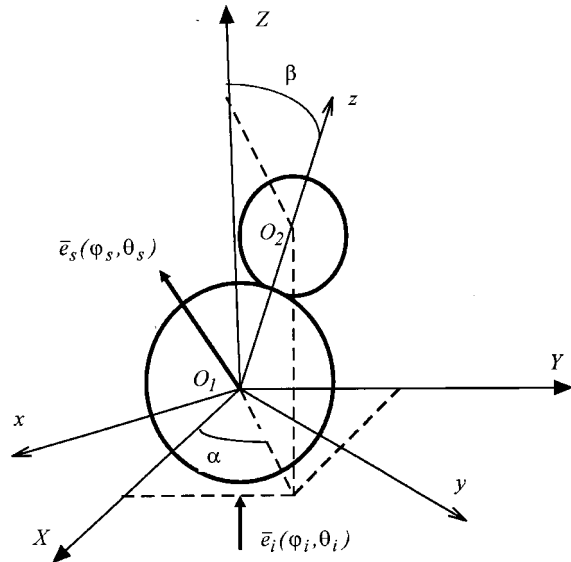


Fig. 1: Geometry of the scattering problem.

In the context of a geometric optics model we assume that the far-zone scattered field is due to the reflection mechanism and that the reflected field sums the contribution of rays emerging from the specular points. Further simplifications are made by neglecting the second-order reflection mechanism and by assuming that there are exactly two specular points A_1 and A_2 , one of each spherical surface as shown in Figure 2.

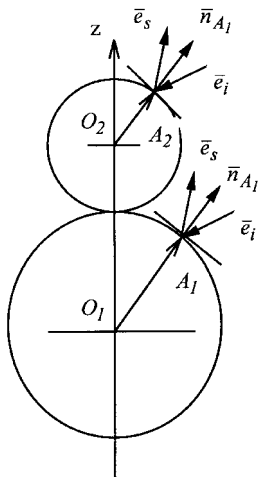


Fig. 2: Geometry of the first-order reflection points (specular points).

Consequently, the far-zone scattered field in the $\mathbf{e}_s(\varphi_s, \theta_s) = \mathbf{r}/r$ direction can be expressed as

$$\mathbf{E}(\mathbf{r}) = \frac{iE_0}{kr} e^{ikr} (S_{ref}^1 e^{i\delta_{ref}^1} + S_{ref}^2 e^{i\delta_{ref}^2}) \mathbf{e}_{ref} \quad (1)$$

where S_{ref} , δ_{ref} and \mathbf{e}_{ref} are the magnitude, the phase and the polarization vector of electric-field contributions, respectively, E_0 is the electric field strength and k is the wavenumber.

The specular points are those points on the spherical surfaces with the unit normal given by $\mathbf{n}_{A_1} = \mathbf{n}_{A_2} = (\mathbf{e}_s - \mathbf{e}_i)/|\mathbf{e}_s - \mathbf{e}_i|$. The magnitude of the reflected electric field is related to the principal radius of curvature of the surface at the specular point [9]. For a two-sphere system the expressions for S_{ref}^1 and S_{ref}^2 simplify to

$$S_{ref}^1 = ka_1/2, \quad S_{ref}^2 = ka_2/2. \quad (2)$$

The phases of the reflected rays are given by [9]

$$\delta_{ref}^1 = -ka_1|\mathbf{e}_s - \mathbf{e}_i| \quad (3)$$

$$\delta_{ref}^2 = k\Delta\mathbf{e}_3 \cdot (\mathbf{e}_s - \mathbf{e}_i) - ka_2|\mathbf{e}_s - \mathbf{e}_i|$$

where \mathbf{e}_3 is the unit vector in the z -direction.

Combining Eqs. (1)–(3), we find that the phase δ_{ref} of the scattered field

$$\mathbf{E}(\mathbf{r}) = \frac{iE_0}{kr} e^{ikr} S_{ref} e^{i\delta_{ref}} \mathbf{e}_{ref} \quad (4)$$

can be formally written as

$$\delta_{ref} = \delta_{ref}(\mathbf{e}_i, \mathbf{e}_s) = \arctan \left(\frac{a_1 \sin \delta_{ref}^1 + a_2 \sin \delta_{ref}^2}{a_2 \cos \delta_{ref}^1 + a_2 \cos \delta_{ref}^2} \right). \quad (5)$$

The above relationship shows that the phase of the scattered field depends on the radii of the spheres a_1 and a_2 and the orientation angles of the z -direction α and β .

In a PDA system, the particle is illuminated by two incident waves travelling in the \mathbf{e}_i^1 and \mathbf{e}_i^2 directions, while the scattered field is analyzed in the \mathbf{e}_s^A and \mathbf{e}_s^B directions. The phase difference between the signals of two point detectors can be simply expressed as

$$\phi_{AB} = \phi_A - \phi_B = [\delta_{ref}(\mathbf{e}_i^1, \mathbf{e}_s^A) - \delta_{ref}(\mathbf{e}_i^2, \mathbf{e}_s^A)] - [\delta_{ref}(\mathbf{e}_i^1, \mathbf{e}_s^B) - \delta_{ref}(\mathbf{e}_i^2, \mathbf{e}_s^B)]. \quad (6)$$

For our numerical investigation we consider an optical configuration with a beam intersection angle of 1.5° , an off-axis angle of 40° and an elevation angle of 8° . The optical parameters are in accordance with the experimental set-up described in Section 4. Since in practical applications the orientation of the axis between the spheres centers is unknown, we organize the phase difference as a random variable. The value of this random variable corresponds to different values of the orientation angles α and β . The frequency of appearance of the random variable phase difference is computed for α in the range $[0, 2\pi]$ and β in the range $[0, \pi]$. Figure 3 shows the relative frequency distribution of the phase difference for the following geometrical configurations of the two-sphere system: (a) $a_1 = 18 \mu\text{m}$, $a_2 = 14 \mu\text{m}$, $\Delta = 32 \mu\text{m}$, (b) $a_1 = 18 \mu\text{m}$, $a_2 = 12 \mu\text{m}$, $\Delta = 30 \mu\text{m}$ and (c) $a_1 = 18 \mu\text{m}$, $a_2 = 10 \mu\text{m}$, $\Delta = 28 \mu\text{m}$.

The most probable phase difference is the peak of the histogram. This peak is pronounced when the size parameters of the spheres are comparable and decreases when the size parameters of the spheres differ significantly. We call by convention the most probable phase difference the phase difference of the ensemble.

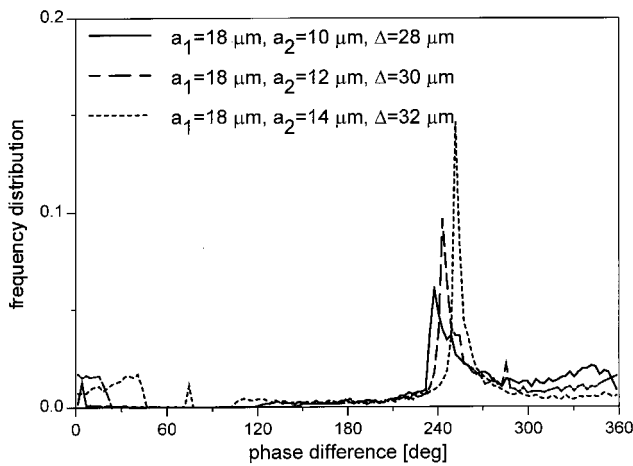


Fig. 3: Relative frequency distribution of the phase difference computed with the specular reflection model. The data correspond to the following geometrical configurations of the two-sphere system: (a) $a_1 = 18 \mu\text{m}$, $a_2 = 14 \mu\text{m}$, $\Delta = 32 \mu\text{m}$, (b) $a_1 = 18 \mu\text{m}$, $a_2 = 12 \mu\text{m}$, $\Delta = 30 \mu\text{m}$ and (c) $a_1 = 18 \mu\text{m}$, $a_2 = 10 \mu\text{m}$, $\Delta = 28 \mu\text{m}$.

3 Geometric Optics Model for Computing the Phase-Doppler Signal

In order to obtain a more accurate description of the phase difference, we extend our geometric optics model for PDA calculations [9] to the two-sphere system. This model removes some simplifications of our above analysis. The main particularities of the geometric optics model can be summarized as follows:

1. for perfectly conducting scatterers the far-zone electric field is derived for diffraction and reflection;
2. the reflected fields sums the contribution of rays which emerge from the specular points if and only if these points are illuminated and in view of the observation point;
3. owing to the concave-convex geometry a second-order reflection at the surfaces is considered. The meaning of the second-order reflection mechanism was discussed in a previous paper [1].

The numerical analysis in Section 2 is reconsidered by using the geometric optics model. The data presented in Figure 4 show that in addition to the phase difference of the ensemble, two peaks appear in the frequency distribution of the phase difference. These peaks correspond to the phase difference of each individual sphere. In this case the scattered ray emerges from a single specular point on the particle surfaces while the other is not visible from the incidence or the observation direction.

We note that when the size parameter of the large sphere becomes much larger than the size parameter of the small sphere, a single peak occurs in the histogram. This is shown in Figure 5, where a two sphere configuration with $a_1 = 18 \mu\text{m}$, $a_2 = 6 \mu\text{m}$ and $\Delta = 24 \mu\text{m}$ is considered. The peak corresponds to the phase difference of the large sphere while the influence of the small sphere consists only in a broadening of the frequency distribution.

The above analysis clearly shows that agglomerated spheres can lead to erroneous results in phase-Doppler anemometry. From an experimental point of view, it is most probable that only a single particle will be detected. Since the frequency of appearance of the phase difference corresponding to the large sphere is higher than the phase differences of the ensemble and of the small sphere, we expect that the size distribution will be shifted to higher particle diameters.

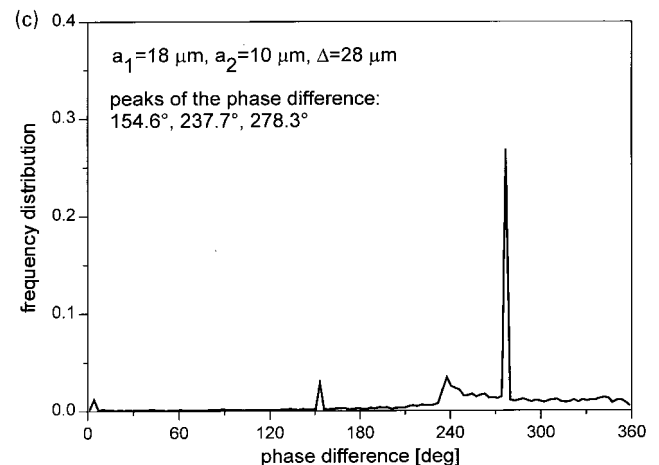
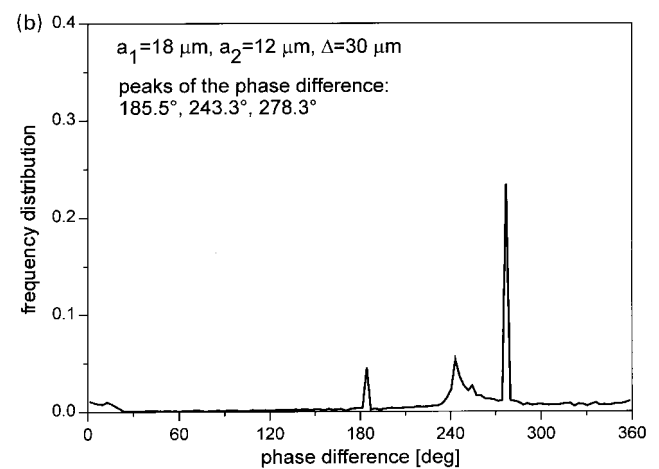
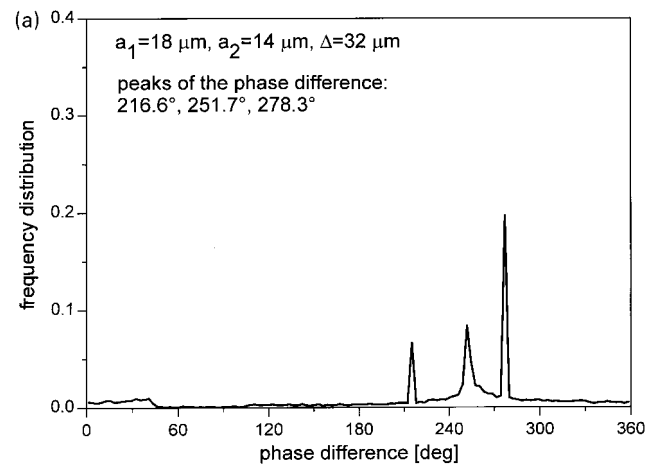


Fig. 4: Relative frequency distribution of the phase difference computed with the geometric optics model. The data correspond to the following geometrical configurations of the two-sphere system: (a) $a_1 = 18 \mu\text{m}$, $a_2 = 14 \mu\text{m}$, $\Delta = 32 \mu\text{m}$, (b) $a_1 = 18 \mu\text{m}$, $a_2 = 12 \mu\text{m}$, $\Delta = 30 \mu\text{m}$ and (c) $a_1 = 18 \mu\text{m}$, $a_2 = 10 \mu\text{m}$, $\Delta = 28 \mu\text{m}$.

4 PDA Measurements

Our experimental set-up consists basically of a two-detector PDA system and an electrodynamic particle trap for the levitation of individual particles.

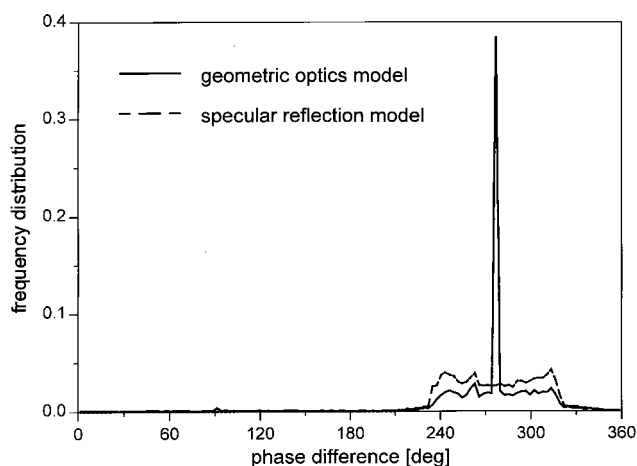


Fig. 5: Relative frequency distribution of a two sphere configuration with $a_1 = 18 \mu\text{m}$, $a_2 = 6 \mu\text{m}$ and $\Delta = 24 \mu\text{m}$.

The light source for the PDA system is a 100 mW argon ion laser at a wavelength of $\lambda = 488 \text{ nm}$. Beam splitting is performed by a radial diffraction grating ($32 \mu\text{m}$ grid separation) for beam splitting and the imaging and focusing of both Gaussian beams is done by an appropriate arrangement of two lenses along the optical track. For the measurements presented below we chose a total beam crossing angle at 3.0° and a beam diameter of $120 \mu\text{m}$. The polarization of the beams was perpendicular with respect to the mean scattering plane. Two individually mounted photomultiplier tubes (PMTs) are used for detection of the scattered light. Their front lenses are of 52 mm aperture and have a focal length of 300 mm . The PMTs are located at an off-axis angle of 40° under 8.0° elevation. Data evaluation is performed by means of a standard FFT algorithm. Details of the set-up have been published by Göbel et al. [10].

Electrodynamic levitation of individual particles is a widely used technique. Gravity is compensated for by supplying a DC field of appropriate strength on an electrically charged particle. A dynamic trapping force is provided by an additional AC field. Our trap is built of four ring electrodes, which are arranged parallel with their centers coinciding with the vertical z -axis of symmetry (direction of gravity). Both solid and fluid particles in the size range ($5 \mu\text{m} < d < 50 \mu\text{m}$) can be carried over sufficiently large periods of time. A trapped particle can be forced to oscillate harmonically in a vertical direction with variable amplitude by adjusting the electric fields. This provides the necessary particle velocity with respect to the beam intersection area. After PDA measurements the levitated particle is captured by means of an electrostatic collector for characterization by an electron microscope. The capturing process and the particle trapping procedure can be observed visually via a Questar telescope and a video system. We should point out that the agglomerate rotates inside the trap during either the oscillation in the vertical direction or the containment. This is obvious from visual observation with the Questar system, when particles with dimensions clearly larger than the resolution of the Questar ($1.5 \mu\text{m}$) are levitated. Under these circumstances different regions of the agglomerate surface will be investigated during the measurement process.

For our PDA measurements we assume that the rotation of the agglomerate is sufficient to put in evidence the three peaks of the phase distribution. Since we do not use a rigorous model for light scattering calculations, we cannot expect a rigorous, theoretical reconstruction of the phase distribution for a fully random orientation of the agglomerate in all directions. Actually, we do

not solve a complex inversion problem consisting of computation of particle sizes and surface roughness. We are mainly interested in identifying the peaks of the phase distribution which are predicted by a simple geometric optics model.

We performed PDA measurements on *Sn63Pb37* alloy (8422 kg/m^3) particles which were produced by ultrasonic standing field dispersion. While trapping individual *Sn63Pb37* particles from a sieved fraction ($20 \mu\text{m} < d < 32 \mu\text{m}$) we happened to levitate an agglomerate of these particles. Figure 6 shows an electron microscope photograph of this particle. As it turned out to be necessary to cover the sample holder with conducting glue in order to yield higher efficiencies of the capturing process, the particle is submerged in this glue to some extent. Nevertheless, the size of the individual spheres can be determined to be $a_1 = 18.8 \mu\text{m}$ and $a_2 = 17 \mu\text{m}$.

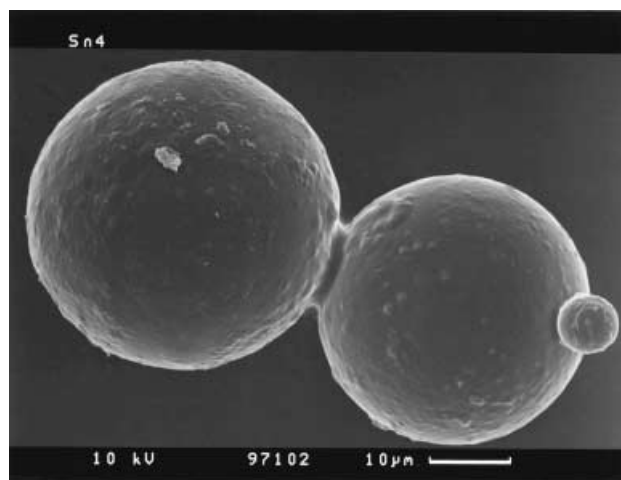


Fig. 6: Electron microscope photograph of the investigated agglomerate.

We performed 10^4 repeated PDA measurements on this agglomerate and the resulting number density of phase differences is depicted in Figure 7. The phase difference distribution shows that there is good agreement between the values of the measured peaks and the theoretical peaks. We note that the broadening of the measured phase difference distribution is due to the surface roughness of each individual sphere. This effect was discussed previously [1].

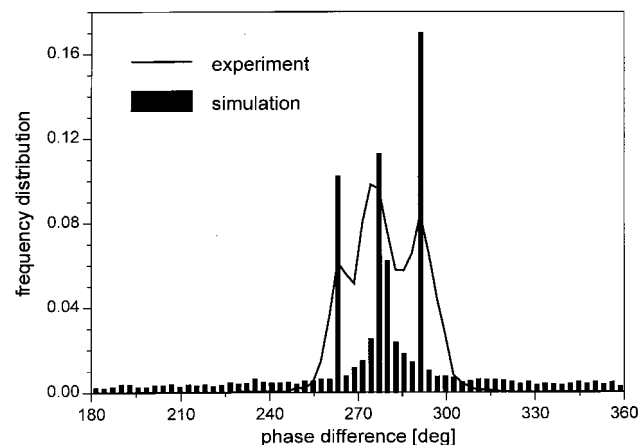


Fig. 7: Measured and simulated phase frequency distributions of the agglomerate.

5 Conclusions

In order to examine the behavior of the signal phase in a phase Doppler system, fundamentals of light scattering from a two-sphere system in the intersection of two laser beams have been discussed. Mathematical tools based on the approximate ray theory have been presented. It has been shown that three peaks appear in the phase difference histogram. These peaks correspond to the phase difference of each individual sphere and to the phase difference of the ensemble. When the size parameter of one sphere becomes much larger than that of the other, a single peak corresponding to the large sphere occurs in the frequency distribution. In this case the influence of the small sphere consists in a broadening of the phase distribution.

From an experimental point of view, we conclude that the impact of agglomerates on the response of a PDA is significant, since only a single particle will be detected. It has been shown that it is most probable that one will detect the particle with the larger size parameters. Consequently, the size distribution is expected to be shifted to higher particle diameters.

6 Symbols and Abbreviations

a_1, a_2	radii of the scattering spheres
\mathbf{E}	scattered field
E_0	electric field strength
\mathbf{e}_s	unit vector of the scattering direction
\mathbf{e}_i	unit vector of the incident direction
\mathbf{e}_{ref}	polarization vector of the resulting scattered field
k	wavenumber
$\mathbf{n}_{A_1}, \mathbf{n}_{A_2}$	normal unit vectors at stationary phase points
S_{ref}^1, S_{ref}^2	magnitude of electric-field contributions
S_{ref}	magnitude of the resulting scattered field
α, β	Euler angles giving the orientation of the symmetry axis of the two-sphere system in the global coordinate system

Δ	distance between spheres centers
$\delta_{ref}^1, \delta_{ref}^2$	phase of electric-field contributions
δ_{ref}	phase of the resulting scattered field
ϕ_{AB}	phase difference between the signals of two point detectors A and B
φ_i, θ_i	angular coordinates of the incident wave vector
φ_s, θ_s	angular coordinates of the scattered wave vector

7 References

- [1] G. Göbel, A. Doicu, T. Wriedt, K. Bauckhage: Influence of surface roughness of conducting spheres on the response of a phase-Doppler anemometer. Part. Part. Syst. Charact. 14 (1997) 283–289.
- [2] W. Trinks: Zur Vielfachstreuung an kleinen Kugeln. Ann. Phys. 22 (1935) 561–590.
- [3] J. H. Bruning, Y. T. Lo: Multiple scattering of EM waves by spheres, Parts I and II. IEEE Trans. Antennas Propagat. 19 (1971) 378–400.
- [4] F. Borghese, P. Denti, G. Toscano, O. I. Sindoni: Electromagnetic scattering by a cluster of spheres. Appl. Opt. 18 (1979) 116–120.
- [5] K. A. Fuller, G. W. Kattawar: Consummate solution to the problem of classical electromagnetic scattering by an ensemble of spheres. II: Clusters of arbitrary configuration. Opt. Lett. 13 (1988) 1063–1065.
- [6] Y. M. Wang, W. C. Chew: A recursive T-matrix approach for the solution of electromagnetic scattering by many spheres. IEEE Trans. Antennas Propagat. 41 (1993) 1633–1639.
- [7] S. Stein: Additional theorems for spherical vector wave functions. Q. J. Appl. Math. 19 (1961) 15–24.
- [8] O. R. Cruzan: Translational addition theorems for spherical functions. Q. J. Appl. Math. 29 (1962) 33–40.
- [9] A. Doicu, T. Wriedt, K. Bauckhage: Light scattering by homogeneous axisymmetric particles for PDA-calculations to measure both axes of spheroidal particles. Part. Part. Syst. Charact. 14 (1997) 3–11.
- [10] G. Göbel, T. Wriedt, K. Bauckhage: Micron and sub-micron aerosol sizing with a standard phase-Doppler anemometer. J. Aerosol Sci. 29 (1998) 1063–1073.